

## Article

# Overexpression of *PvFAD3* Gene from *Plukenetia volubilis* Promotes the Biosynthesis of $\alpha$ -Linolenic Acid in Transgenic Tobacco Seeds

Guo Liu \*, Zhihua Wu, Xiuhua Shang, Yan Peng and Liqiong Gao

Research Institute of Fast-Growing Trees, Chinese Academy of Forestry, 30 Mid Renmin Avenue, Zhanjiang 524022, China; cercwuzhua2889@caf.ac.cn (Z.W.); cercshxh@caf.ac.cn (X.S.); cercpengy@caf.ac.cn (Y.P.); riftgaolq@caf.ac.cn (L.G.)

\* Correspondence: cereliug@caf.ac.cn

**Abstract:** The  $\omega$ -3 fatty acid desaturase (*FAD3*) gene encodes a rate-limiting enzyme in the synthesis of  $\alpha$ -linolenic acid. In this study, homologous cloning was used to obtain the full-length sequence of the *PvFAD3* gene of *Plukenetia volubilis*. The full-length DNA sequence was 1871 bp long, with 8 exons and 7 introns. The structural analysis of the amino acid sequence revealed that the *PvFAD3* protein contained three histidine-conserved regions and an endoplasmic reticulum retention signal. The real-time reverse transcription-polymerase chain reaction performed for determining the expression patterns of the *PvFAD3* gene in different tissues of *P. volubilis* showed that *PvFAD3* expression was highly expressed in the fast oil accumulation stage of seed. The analysis of subcellular localization assay in epidermal cells of tobacco (*Nicotiana benthamiana*) leaves showed that the *PvFAD3* protein was mainly localized in the endoplasmic reticulum. Seed-specific overexpression vectors were constructed, and *Agrobacterium*-mediated genetic transformation was performed to obtain transgenic tobacco plants overexpressing *PvFAD3*. The results of fatty acid assays performed using harvested seeds showed a significant increase in  $\alpha$ -linolenic acid content, a dramatic decrease in linoleic acid content, and an obvious increase in oil content in transgenic tobacco seeds. Collectively, the *PvFAD3* gene of *P. volubilis* was confirmed as a key enzyme gene for  $\alpha$ -linolenic acid synthesis; thus, indicating that the *PvFAD3* gene can be used for fatty acid fraction improvement in oilseed plants.

**Keywords:** *Plukenetia volubilis*; *PvFAD3*; expression pattern; subcellular localization; overexpression



**Citation:** Liu, G.; Wu, Z.; Shang, X.; Peng, Y.; Gao, L. Overexpression of *PvFAD3* Gene from *Plukenetia volubilis* Promotes the Biosynthesis of  $\alpha$ -Linolenic Acid in Transgenic Tobacco Seeds. *Genes* **2022**, *13*, 450. <https://doi.org/10.3390/genes13030450>

Academic Editor: Mingli Wang

Received: 10 February 2022

Accepted: 25 February 2022

Published: 28 February 2022

**Publisher's Note:** MDPI stays neutral with regard to jurisdictional claims in published maps and institutional affiliations.



**Copyright:** © 2022 by the authors. Licensee MDPI, Basel, Switzerland. This article is an open access article distributed under the terms and conditions of the Creative Commons Attribution (CC BY) license (<https://creativecommons.org/licenses/by/4.0/>).

## 1. Introduction

*Plukenetia volubilis* L. is a perennial woody vine of the Euphorbiaceae family, which can produce fruits in the same year of planting and within 2–3 years after it enters the productive period of up to 10 years, with great economic value [1]. With an oil content of 35% to 60% [2], *P. volubilis* seeds are free from any toxins and harmful substances and contain more than 90% unsaturated fatty acids. This makes them one of the vegetable oils with the highest unsaturated fatty acid content worldwide, with a ratio of 1:0.75 for  $\omega$ -3: $\omega$ -6 unsaturated fatty acids, which is closest to the absorption ratio of the human body as one of the best edible oils [3,4]. *P. volubilis* seeds contain 35.60% of  $\alpha$ -linolenic acid, next to flaxseed and perilla seed in acid content, and are one of the main sources of  $\alpha$ -linolenic acid product development [5,6].

$\alpha$ -Linolenic acid (C18:3, ALA) is an essential, plant-based,  $\omega$ -3 polyunsaturated fatty acid that is obtained through the diet. It is a precursor for synthesizing two essential factors (EPA, C20:5, and DHA, C22:6) in the human body [7,8]. The synthesis and accumulation of  $\alpha$ -linolenic acid are closely related to the *FAD3* gene, and the synthesis of  $\alpha$ -linolenic acid in plant seeds is catalyzed by the *FAD3* protein for linoleic acid in the endoplasmic reticulum [9]. Several studies have reported that *FAD3* overexpression can significantly increase  $\alpha$ -linolenic acid content in leaves, roots, fruits, seeds, and other

tissues of *Arabidopsis thaliana* [10], *Brassica napus* [11], and *Lycopersicon esculentum* [12]. The FAD3 gene has been successfully cloned and expressed in various plants, including *Glycine max* [13], *B. napus* [11], *Jatropha curcas* [14], *Arachis hypogaea* [15], *Erilla frutescens* [16], *Paeonia suffruticosa* [17], and *Camellia sinensis* [18]. In most plants, the FAD3 gene is highly expressed in seeds, and the expression is closely related to  $\alpha$ -linolenic acid synthesis in seeds. For instance, the *JcFAD3* gene was overexpressed in *A. thaliana* seeds, in which the  $\alpha$ -linolenic acid level was significantly increased by 20.50% to 24.94% compared to wild-type seeds [14]. Specific expression of the *FAD3c* gene of *G. max* in sesame seeds resulted in a 4.91% increase in the specificity of  $\alpha$ -linolenic acid levels in sesame seeds [19]. The vector with *EuFAD3-1* overexpression increased the  $\alpha$ -linolenic acid content of transgenic tobacco seeds by 4.27% after transfer into tobacco [20]. Our research team analyzed the transcriptomic data of *P. volubilis* seeds at various growth stages obtained using second-generation high-throughput sequencing technology and discovered that the *PvFAD3* gene in *P. volubilis* seeds was overexpressed during the rapid period of oil accumulation. [21]. We presumed that the extremely high expression level of *PvFAD3* was closely related to the efficient accumulation of  $\alpha$ -linolenic acid, which is consistent with the findings of Wang et al. [22,23] on *P. volubilis* seeds.

In this study, we aimed to characterize the expression patterns further. Biological functions of the *PvFAD3* gene in *P. volubilis* were selected to clone the full-length coding sequence of the *PvFAD3* gene, and the sequence structure was analyzed by bioinformatics analyses. Real-time reverse transcription-polymerase chain reaction (qRT-PCR) was performed to assess the expression of the gene in different tissues of *P. volubilis*. The expression of the *PvFAD3* gene was also characterized by subcellular localization. Seed-specific overexpression vectors were constructed, and *Agrobacterium*-mediated genetic transformation was performed to obtain transgenic tobacco plants overexpressing the *PvFAD3* gene. This study provides a basis for further understanding of the synthesis and metabolic mechanism of  $\alpha$ -linolenic acid in oil plants and lays a theoretical foundation for improving the seed oil composition to get high yield and high quality oil plants.

## 2. Materials and Methods

### 2.1. Materials

Three-year-old *P. volubilis* plants were grown in the South China Experimental Nursery, located in Zhanjiang City in the southwest of Guangdong Province, China. Fresh leaves were used as the material for extracting genomic DNA and RNA. *Nicotiana benthamiana* ( $2n = 38$ ) was used for the subcellular localization and plant transformation as the test material.

### 2.2. Cloning of the DNA Sequence of the *PvFAD3* Gene

The genomic DNA of *P. volubilis* was extracted using the modified CTAB method, and the integrity of the genomic DNA was examined using 1% agarose gel electrophoresis. Full-length cDNA and genomic sequences of *PvFAD3* were amplified from *P. volubilis* with FAD3-F and FAD3-R (Supplementary Table S1) as primers. The primers were designed based on the transcript sequence of the *PvFAD3* (Unigene0043398) in *P. volubilis* seed transcriptome (SRR8205220). The PCR reaction system included 1.5  $\mu$ L of the forward primer, 1.5  $\mu$ L of the reverse primer, 25  $\mu$ L of 2 $\times$  Ex Taq buffer, 1  $\mu$ L of dNTP (10 mmol $\cdot$ L<sup>-1</sup>), 5  $\mu$ L of cDNA, 1  $\mu$ L of Ex Taq enzyme (5 U/ $\mu$ L, TaKaRa Bio, Beijing, China), and 15  $\mu$ L of ddH<sub>2</sub>O. The reaction procedure was as follows: pre-denaturation at 94 °C for 2 min, denaturation at 94 °C for 30 s, annealing at 53 °C for 30 s, extension at 72 °C for 1 min, for 35 cycles; hold at 72 °C for 10 min, store at 4 °C. The PCR products were subjected to agarose gel electrophoresis, recovered, ligated into the pMD19-T vector (Takara, Dalian, China), and sequenced by transforming the positive clones obtained from *Escherichia coli*.

### 2.3. Bioinformatics Analysis

Splign, a spliced-alignment tool in NCBI, was used to analyze the structure of *PvFAD3*. Theoretical isoelectric point (pI) and molecular weight of *PvFAD3* were predicted by Ex-

PASy ([http://web.expasy.org/compute\\_pi/](http://web.expasy.org/compute_pi/), accessed on 12 November 2021). Multiple sequence alignment was performed using Bioedit 7.0. A phylogenetic tree of PvFAD3 and other  $\omega$ -3 fatty acid dehydrogenase was constructed by PhyML 3.0 software (maximum likelihood method), and bootstrap analysis using 1000 replicates. The analysis of transmembrane protein structure was carried out using TMHMM Server V2.0 (<http://www.cbs.dtu.dk/services/TMHMM/>, accessed on 9 November 2021). The secondary structure and tertiary structure models of submits of PvFAD3 protein were predicted using Phyre v2.0 (<http://www.sbg.bio.ic.ac.uk/phyre2/>, accessed on 18 November 2021).

#### 2.4. Expression Pattern of PvFAD3 Gene

Primer 6.0 was used to design the qRT-PCR primers (Unigene0043398-F and Unigene0043398-R) (Supplementary Table S1), and total RNA was extracted from the samples using an RNAPrep pure plant kit (TIANGEN, Beijing, China) and reverse transcribed using a HiScript II Q RT SuperMix for qPCR (+gDNA wiper) (Vazyme, Nanjing, China). The RNA quality for all samples was assessed by NanoDrop 2000 spectrophotometer (Thermo Fisher, Waltham, MA, USA). The qRT-PCR amplifications were performed with a Thermo Scientific PikoReal 96 Real-Time PCR System using iQ SYBR Green Supermix (TaKaRa Bio, Beijing, China) according to the manufacturer's instructions. PCR product specificities were confirmed by melt curve analysis. Triplicate samples of qRT-PCR for PvFAD3 were prepared in a total volume of 20  $\mu$ L that contained 4  $\mu$ L cDNA template, 10  $\mu$ L 2 $\times$  ChamQ SYBR qPCR Master Mix (Vazyme, Nanjing, China) and 0.4  $\mu$ L in forward and reverse primers. The actin gene (Unigene0042747) was used as an internal reference standard. The PCR reaction procedure was as follows: predenaturation at 95  $^{\circ}$ C for 1.5 min, denaturation at 95  $^{\circ}$ C for 5 s, annealing at 60  $^{\circ}$ C for 15 s, extension at 72  $^{\circ}$ C for 20 s, for 40 cycles; hold at 72  $^{\circ}$ C for 10 min, store at 4  $^{\circ}$ C. Statistical analyses were performed using the  $2^{-\Delta\Delta C_t}$  method [24] (Livak & Schmittgen 2001) to calculate the relative expression of the *PvFAD3* gene in the root, stem, leaf (Mature leaf and Young leaf), pericarp, and seeds (the initial stage, Pv-1, and the fast oil accumulation stage, Pv-2) of *P. volubilis*, and multiple comparisons were performed using the Q-test, and significant differences were analyzed by a range test (significant differences at  $p < 0.05$ ).

#### 2.5. Construction of Fusion Vector and Overexpression Vector

The RNA prep pure plant kit (TIANGEN, Beijing, China) was used to extract total RNA, and then it was reverse transcribed into cDNA using the PrimeScript<sup>TM</sup> RT reagent kit (TaKaRa Bio, Beijing, China). The *PvFAD3* gene transcript sequence was used to create primers to construct a subcellular localization vector (YFP-FAD3-F and YFP-FAD3-R, Supplementary Table S1), and the cDNA was used as a template for PCR. The amplification product was cloned by homologous recombination into the EcoRI and SpeI sites of the vector p131-YFP to generate the expression vector of the fusion protein p131-PvFAD3-YFP.

The primers of the overexpression vector were designed on the basis of the sequence of Unigene0043398 (1301-FAD3-F and 1301-FAD3-R, Supplementary Table S1). Using the p131-PvFAD3-YFP plasmid as a template, the ORF (Open reading frames) sequence of the *PvFAD3* gene was amplified, and the PCR amplification product was cloned into BglII and BstEII of the expression vector pCAMBIA1301 by homologous recombination to replace the GUS ( $-\beta$ -Glucuronidase) gene in the vector. The target fragment was recovered using 1% agarose gel electrophoresis and ligated to a large fragment of the pCAMBIA1301 vector T4-DNA Ligase and incubated overnight at 4  $^{\circ}$ C. The ligated product was transferred to *E. coli* Top10 receptor cells using heat-shock transformation and coated on LB plates containing kanamycin (Kan) and incubated overnight at 37  $^{\circ}$ C. Positive clones were screened, and recombinant plasmids were extracted and identified using enzymatic digestion. The vector pCAMBIA1301-PvFAD3 was created.

### 2.6. Subcellular Localization

The constructed subcellular localization vector plasmid was transformed with *Agrobacterium tumefaciens* GV3101, and p131–35S-YFP empty vector used as a control was set up. After incubating overnight, *Agrobacterium* was harvested by centrifugation and suspended in a suspension solution composed of 10 mM MgCl<sub>2</sub>, 10 mM MES, and 100 μM acetosyringone (AS). It was then mixed with *A. tumefaciens* containing an ER-mCherry subcellular marker plasmid [25], and then infiltrated into tobacco leaves at the 4-to 5-leaf stage after incubation for 3 h at room temperature. The colonies were identified by PCR without error and subjected to *A. tumefaciens* injection of *N. benthamiana* leaves. The expression and distribution of fluorescent proteins in epidermal cells of tobacco leaves were observed 3–5 days after the infiltration using a Leica TCS SP8 (Leica Microsystems GmbH, Wetzlar, Germany) at an excitation wavelength of 514 nm (YFP) and 587 nm (mCherry).

### 2.7. Generation of Transgenic Tobacco and the Determination of Fatty Acid Composition

The overexpression vector pCAMBIA1301-PvFAD3 was used to obtain transgenic tobacco by leaf disc-mediated genetic transformation in *A. tumefaciens*. A pair of specific primers was designed on the basis of the pCAMBIA1301-PvFAD3 vector sequence (35S-F and FAD3-R2(562), Supplementary Table S1), and PCR was performed by using the leaf genomic DNA of wild type and transgenic tobacco as templates. The PCR results were verified by 1.0% agarose gel electrophoresis, and transgenic plants were obtained. Gas chromatography was used to determine the fatty acid composition of mature seeds from transgenic plants and wild tobacco (Agilent 7890A, Palo Alto, CA, USA). The specific operation method used was the same as that used by Liu et al. [26].

## 3. Results

### 3.1. Cloning and Sequence Analysis of the PvFAD3

The genomic DNA and full-length cDNA sequence of *PvFAD3* were successfully cloned from *P. volubilis* on the basis of the Unigene0043398 transcript sequence. The sequence analysis showed that *PvFAD3* had a full length of 1871 bp ORF (Figure 1A). Comparison of the *PvFAD3* cDNA sequence with the transcript sequence of Unigene0043398 indicated that the *PvFAD3* gene contained eight exons, and the genomic DNA fragment was interrupted by seven introns at the 'GT' and 'AG' sites. The length of eight exons ranged from 67 to 290 bp with an average length of 142 bp, whereas the length of the seven introns ranged from 71 to 212 bp with an average length of 105 bp. In the introns, the (A+T) content was 65.53%, and the (G+C) content was 34.47, which is consistent with the higher AT content than GC content in the intron region. NCBI Blast search yielded the protein ID number QGR25673.1, and the sequence of *PvFAD3* had high similarity to the other 34 plants ω-3 fatty acid dehydrogenases, ranging from 73.58% to 87.07% (Supplementary Table S2), with the highest similarity (87.07%) to the ω-3 fatty acid dehydrogenase of *Ricinus communis*, which is also a member of the Euphorbiaceae family.

*PvFAD3* had a 1140 bp ORF encoding 379 amino acids with a molecular weight of 43.53 kD, as deduced by the sequence analysis. The predicted protein's theoretical isoelectric point was calculated to be 7.79, and the stability coefficient was 34.07, indicating that the protein was stable. The hydrophilicity value of the protein was −0.102, indicating that it was hydrophobic. The protein with the aliphatic amino acid coefficient of 92.80 was aliphatic. According to the prediction of the transmembrane domain of *PvFAD3* protein, three transmembrane domains were found (Figure 1B), and the corresponding transmembrane positions were I56–79O205–228I232–255O ("O" means outside the membrane and "I" means inside the membrane). Further analysis revealed that *PvFAD3* did not have a signal peptide splicing site at the N-terminal, indicating that the *PvFAD3* protein probably was located in the endoplasmic reticulum, and the protein may not be secreted to other sites across the membrane.

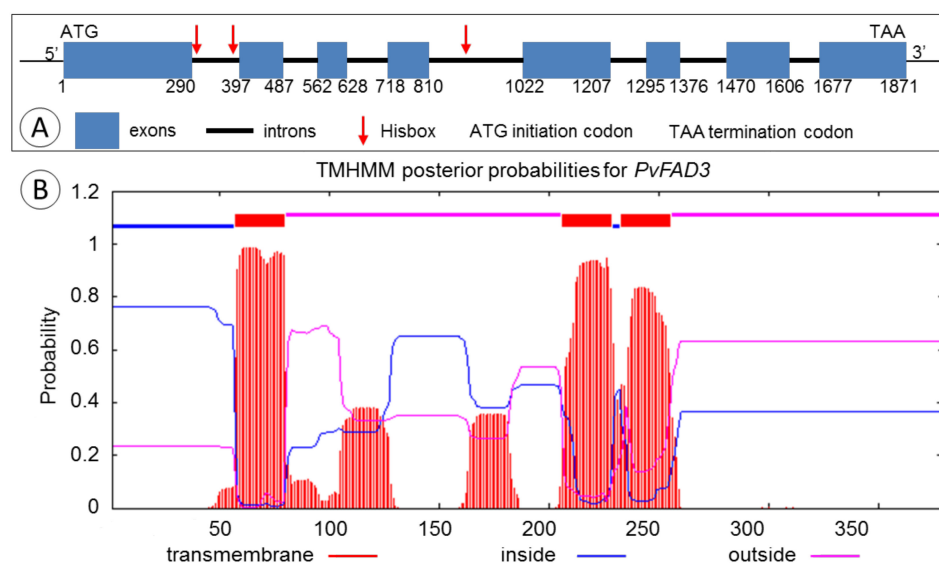


**Figure 1.** (A) Genomic structure of *PvFAD3* gene. The blue bars represent exons. Thick black lines represent introns, red arrows represent hisbox, ATG indicates initiation codon, and TAA indicates termination codon; (B) The transmembrane helix antenna analysis of *PvFAD3*. The red lines indicate transmembrane, blue lines indicate inside and pink lines indicate outside.

The amino acid sequence alignment of *PvFAD3* with the other 34 species of homologous proteins showed that all  $\omega$ -3 fatty acid dehydrogenases (FAD3) contained three typical conserved histidine-rich structural domains, namely HDCGHG (Hisbox I), PYXGWRISHRTHH (Hisbox II), and HHXIGTHVIHH (Hisbox III) (Figure 2), located at amino acids 95–99, 123–135 and 298–302, respectively (Figure 1A). These three histidine-conserved structural domains had a typical amino acid sequence of fatty acid dehydrogenases on the plasma membrane, which mainly formed the active center of the enzyme and bonded with the 2-valent iron ion to participate in the catalytic action of the enzyme [27]. Of the three histidine-conserved structural domains, the conserved motif of Hisbox I was identical in 35 plant species, and the Hisbox II was “PYXGWRISHRTHH” in 24 plants, whereas “PYNGWRISHRTHH” in six species of *Rosaceae* and two species of *Humulus*, and “PYHGWRISHRTHH” in two species of Flax and Cassia. The conserved motif for Hisbox III was “HHXIGTHVIHH” in 34 species, except for *Durio zibethinus* (“HHNIGTHVIHH”).

The C-terminus of the peptide chain of endoplasmic reticulum retention proteins contain a specific amino acid sequence, the sequence in the membrane proteins is “Lys-Lys-X-X” (KKXX) motif, and “Lys-Asp-Glu-Leu” (KDEL) motif are in the soluble proteins [28]. According to the results of the alignment analysis of amino acid sequence (Figure 2), the FAD3 amino acid sequences of 35 plant species differed considerably at the C-terminus, with only *P. volubilis* and *R. communis* having a consistent and specific endoplasmic reticulum retention signal “KKLA” at the C-terminus. In addition, the other 18 sequences of FAD3 all had the KXXK motif at the C-terminus. Also, 35 FAD3 amino acid sequences were rich in aromatic amino acids such as phenylalanine (Phe, Y) and Tyroxine (Tyr, Y) at the C-terminus.

The prediction results of the secondary structure of the *PvFAD3* amino acid sequence (Figure 3A) showed that the *PvFAD3* contained a large number of  $\alpha$ -helices (43.27%) and random coil (39.05%), which may be related to the transmembrane properties of the *PvFAD3*. Additionally, the extended strand was 12.66%, and the  $\beta$ -sheet was 5.01%. The tertiary structure of the *PvFAD3* protein was predicted by homology modeling (Figure 3B), and 250 residues (66% of amino acid sequence) have been modeled with 99.9% confidence by the single highest scoring template.

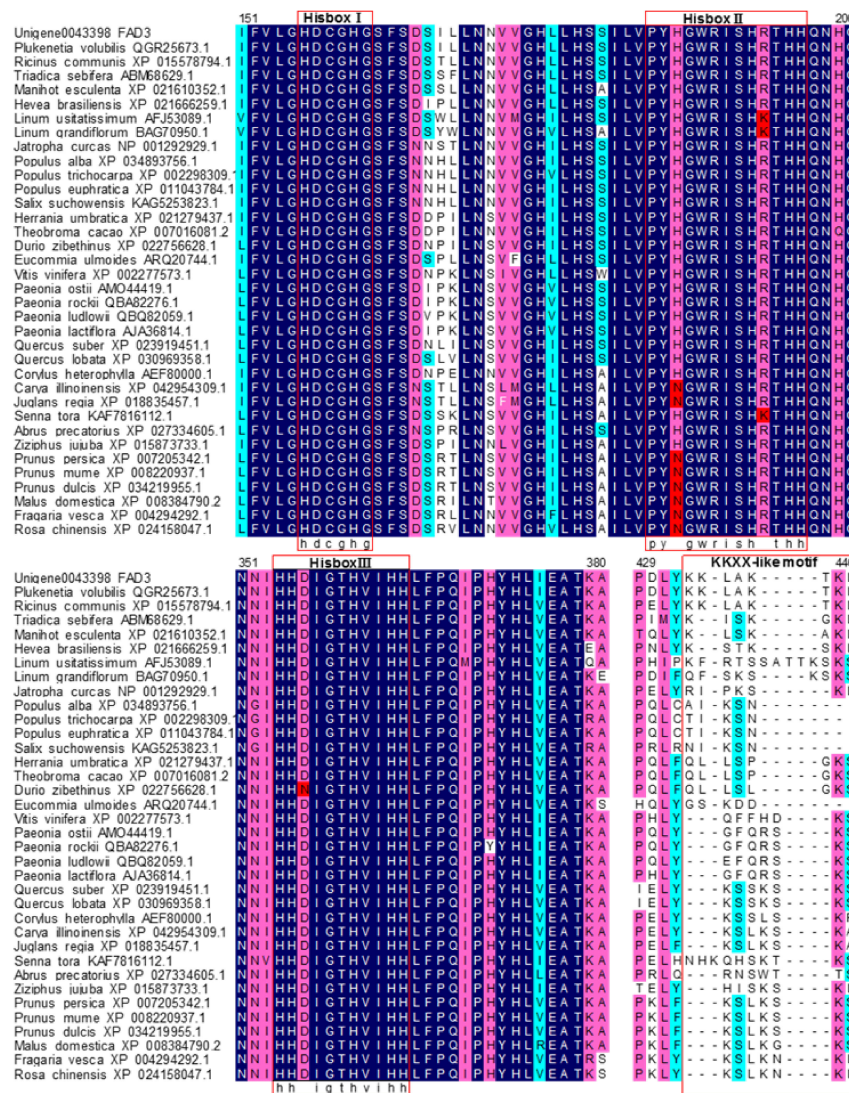


**Figure 2.** The alignment result of FAD3 amino acid sequences. The red boxes indicate Hisbox I, Hisbox II, Hisbox III, and KKXX-like motif, respectively.

The amino acid sequences of PvFAD3 and the other 35  $\omega$ -3 fatty acid dehydrogenases (FAD3) from other plant species were used to build a phylogenetic tree using the maximum likelihood method, with three  $\omega$ -6 fatty acid dehydrogenases (FAD2) from *A. hypogaea*, *Sesamum indicum*, and *G. max* serving as outgroups (Figure 4). The amino acid sequence of PvFAD3, which was cloned in this study, was the closest to the evolutionary relatives of six species from the Euphorbiaceae family and was clustered into a small group. The FAD3 amino acid sequences of four Salicaceae species were more homologous and clustered into a small group. The amino acid sequences from three species of Malvaceae and four species of Paeoniaceae clustered into one large group with *Eucommia ulmoides* and *Vitis vinifera*, of which three species of Malvaceae had closer evolutionary affinities and clustered into a small group. The amino acid sequences of four species of Paeoniaceae were more homologous. The other 14 plants with higher homology of FAD3 amino acids clustered into one group, with plants in the same family and genus having a higher relationship for the FAD3 protein. The two plants in Fabaceae clustered into a small group, two plants in Fagaceae into a small group, and two plants in Juglandaceae into a small group. Six Rosaceae species had higher homology for the FAD3 amino acid sequences. To conclude, the FAD3 amino acid sequences differed among species, and the evolutionary relationship of the FAD3 proteins is higher between species from the same family.

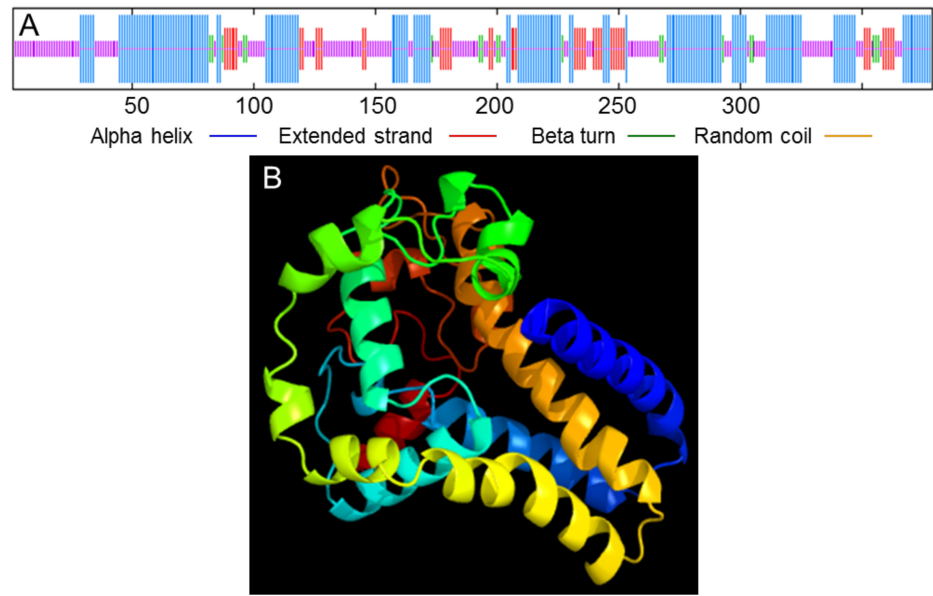


**Figure 3.** (A) Prediction of the secondary structure of PvFAD3 protein. Blue represents alpha helix, red represents extended strand, green represents beta-turn, and yellow represents random coil. (B) Tertiary structure models of submits of PvFAD3 protein based on the model of template c4zyoA.

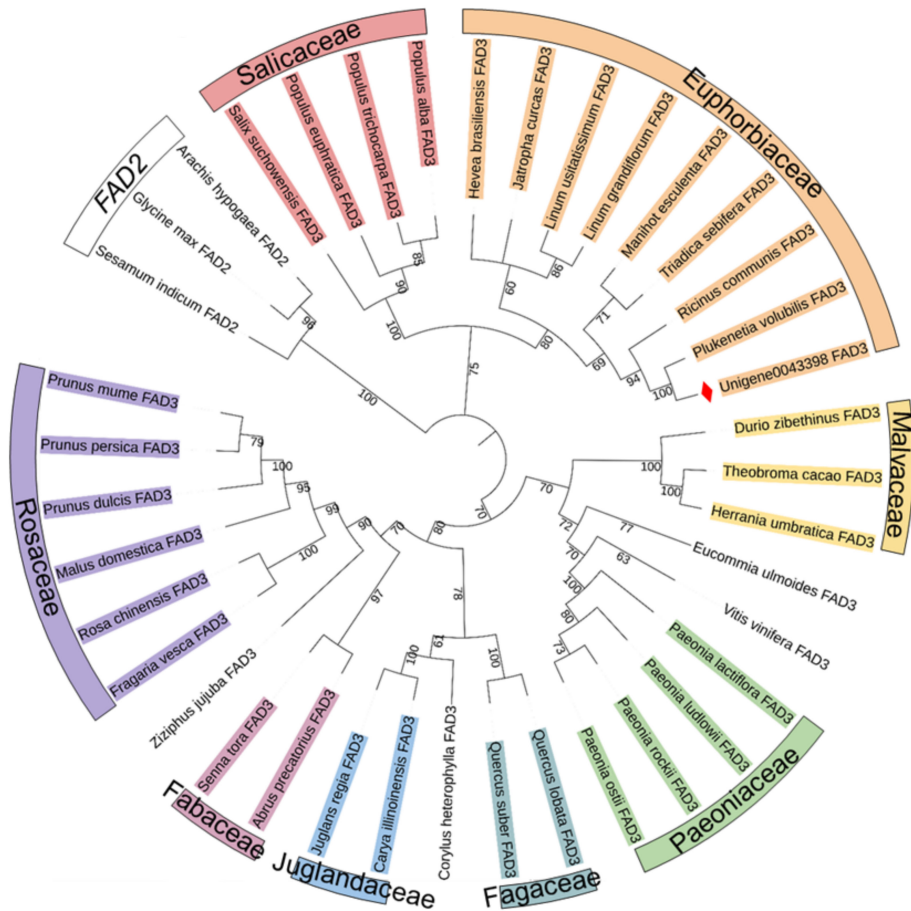


**Figure 4.** Phylogenetic tree of PvFAD3 and FAD3 from other plants. The phylogenetic tree was constructed by PhyML software with the ML method (1000 bootstrap). The red diamond-shape indicates the position of PvFAD3.

### 3.2. Expression Pattern of *PvFAD3* in Different Tissues

The expression pattern of the *PvFAD3* in different tissues of *P. volubilis* was analyzed by qRT-PCR (Figure 5), and the relative expression was calculated using the reference gene (Unigene0042747), which showed that *PvFAD3* was expressed in seven different tissues. It was highly expressed during the fast oil accumulation stage of seed development, and its relative expression was 14.83- and 15.27-times higher than that in the initial stage of seed development, and 14.83- and 15.27-times higher than that in young leaves and roots. The *PvFAD3* gene was least expressed in the mature leaves of *P. volubilis*, followed by a lower expression in the pericarp. The expression analysis of photosynthetic and nonphotosynthetic tissues indicated that *PvFAD3* expression was significantly higher in nonphotosynthetic tissues (roots) than in photosynthetic tissues (mature leaves and pericarp) ( $p < 0.05$ ). Compared with the roots, young leaves with vigorous photosynthesis exhibited no difference in the relative expression of the *PvFAD3* gene.

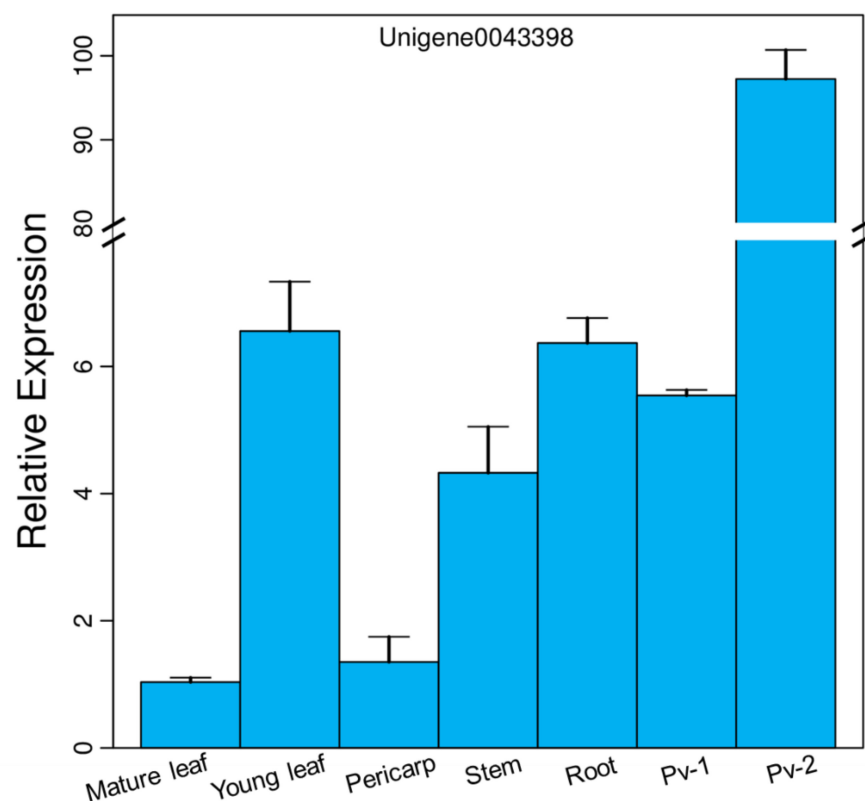


**Figure 5.** The expression patterns of *PvFAD3*. Error bars represent standard error derived from three replicates. The same letters in the figure represent no significant differences, while different letters indicate significant differences. The data were subjected to Student's *t*-test.

### 3.3. Subcellular Localization of *PvFAD3*

To determine the subcellular localization of *PvFAD3* protein, the *PvFAD3* gene was cloned into the EcoRI and SpeI sites of the p131-YFP vector by homologous cloning to generate a p131-*PvFAD3*-YFP fusion vector (Figure 6A). The fusion vector was introduced into *A. tumefaciens* GV3101, the positive clone was picked, and PCR was performed using primers containing the enzyme cut site to obtain a band of the same size as the fragment of *PvFAD3*, which was sequenced. The p131-*PvFAD3*-YFP recombinant plasmid with the correct sequencing result was selected and introduced into the lower epidermis of tobacco leaves by injection. After three days of incubation, the transient expression of the *PvFAD3* gene was observed in the epidermal cells of the leaves of tobacco using Leica TCS SP8.



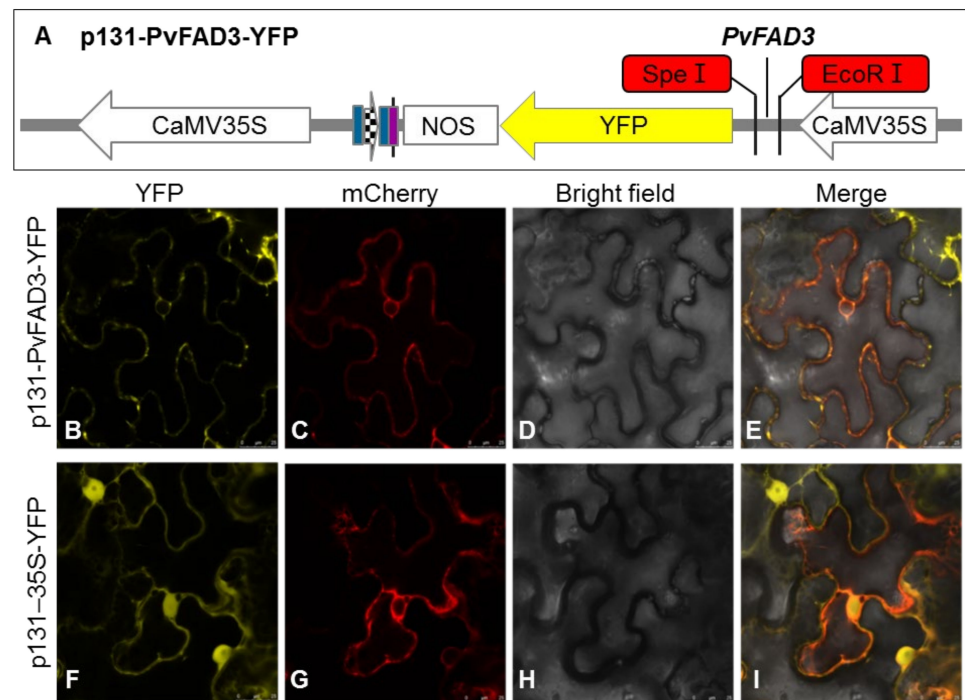


**Figure 6.** (A) Plant fusion vector construction of p131-PvFAD3-YFP; (B–I) Subcellular localization analysis of PvFAD3 fusion protein in leaf epidermal cells of *N. benthamiana*; (B,E) YFP field; (C,G) red field; (D,H) bright field; (E,I) merged pictures. p131-PvFAD3-YFP indicates the fusion protein with PvFAD3, and p131-35S-YFP indicates the empty vector.

The confocal microscopic analysis showed that the yellow fluorescence from *N. benthamiana* leaves infiltrated with *Agrobacterium* containing p131-PvFAD3-YFP fusion vector was observed mainly in the endoplasmic reticulum when using an ER-rk CD3-959 as an ER marker [25] (Figure 6B), whereas the free YFP signal from *N. benthamiana* leaves infiltrated with *Agrobacterium* containing p131-35S-YFP as the control was diffusely distributed throughout the plasma membranes and organelles (Figure 6F). At the excitation wavelength of 587 nm, the red fluorescence of plasma membrane localization protein (mCherry) was normal (Figure 6C,G). After fusing the YFP, mCherry, and Bright fields, the yellow fluorescence of p131-PvFAD3-YFP fusion vector and red fluorescence of mCherry overlapped and turned orange (Figure 6E). Thus, the PvFAD3 protein was mainly located in the endoplasmic reticulum in cells.

### 3.4. Fatty Acid Analysis of *PvFAD3* Gene-Transformed Tobacco Seeds

To understand the physiological functions of the *PvFAD3* gene, the ORF fragment of the gene was amplified using the constructed p131-PvFAD3-YFP plasmid as a template, and the PCR product was cloned into the BglII and BstEII restriction enzyme cutting sites of the pCambia1301 vector by homologous recombination (Figure 7A). After transformation using *A. tumefaciens*, positive clones were selected and analyzed by PCR using primers containing the restriction enzyme cutting site to obtain bands consistent with the fragment size of PvFAD3 (Supplementary Figures S1 and S2). The recombinant pCambia1301-PvFAD3 plasmid was sequenced to confirm its sequence and then used to obtain transgenic tobacco seedlings overexpressing the *PvFAD3* gene via *A. tumefaciens*-mediated genetic transformation by the tobacco leaf disc method (Supplementary Figure S3A–D). Wild-type and positive transgenic tobacco leaves were used as materials for PCR using specific primers (35S-F/FAD3-R2(562)), respectively. The results showed that 13 transgenic tobacco seedlings numbered 2–9, 11–14, and 16 contained the *PvFAD3* gene (Supplementary Figure S3E).

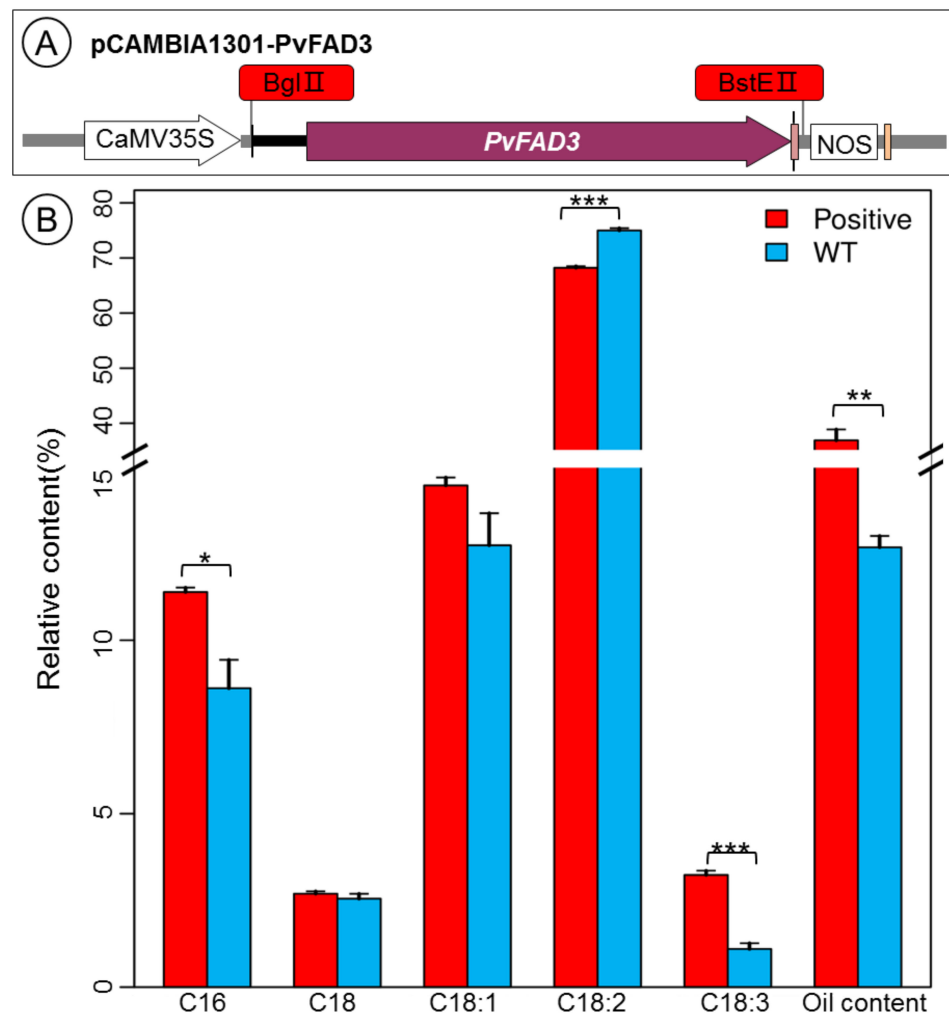


**Figure 7.** (A) The construction of overexpression vector; (B) The main fatty acid content analysis of positive transgenic and wild-type tobacco seeds. Positive represents positive transgenic tobacco seeds, WT represents wild-type tobacco seeds. The difference significance was analyzed by ANOVA. \* represents significant difference at  $p < 0.05$ ; \*\* represents significant difference at  $p < 0.01$ , and \*\*\* represent significant difference at  $p < 0.001$ .

Mature tobacco seeds were harvested from wild-type, 13 positive transgenic tobaccos were grown in a greenhouse under normal light and water, and the fatty acid composition in mature seeds of wild-type and positive transgenic tobacco was analyzed using gas chromatography (Figure 7B). Compared with the wild type, the fatty acid composition was changed greatly in the transgenic tobacco seeds. In particular, the content of alpha-linolenic acid was remarkably higher in positive transgenic tobacco seeds than in wild-type ( $p < 0.001$ ). Simultaneously, oil content ( $p < 0.01$ ) and palmitic acid content ( $p < 0.05$ ) were also increased significantly in positive transgenic tobacco seeds compared with wild-type, separately. Conversely, linoleic acid content was significantly lower in positive transgenic tobacco seeds than in wild-type ( $p < 0.001$ ). These results show that the overexpression of the *PvFAD3* in tobacco could significantly enhance the conversion of linoleic acid to  $\alpha$ -linolenic acid and increase the oil content of the transgenic tobacco seeds.

#### 4. Discussion

$\alpha$ -Linolenic acid is an essential  $\omega$ -3 fatty acid for human growth and development, as it promotes brain development, prevents neurological and cardiovascular diseases, lowers blood lipids, and slows the aging process [29]. In daily life,  $\alpha$ -linolenic acid is relatively

low in traditional diets such as peanuts, soybeans, maize, oil tea, and olives [30], and the balance of fatty acid fractions concerns genetic improvement of oilseed plants.

With the continuous development of oil plants, special oil plants rich in  $\alpha$ -linolenic acid such as *Perilla frutescens* [31], *Salvia hispanica* [32], *Linum usitatissimum* [33], *P. volubilis* [34], and *P. suffruticosa* [35] seeds have been discovered as new sources of  $\alpha$ -linolenic acid and dietary supplements. The high yield and oil content of *P. volubilis* seeds, rich in both  $\alpha$ -linolenic acid and linoleic acid, exhibit greater advantages than those of other oil plants and have greater potential for exploitation. The cloning, expression, and functional analysis of PvFAD3, a key enzyme for  $\alpha$ -linolenic acid biosynthesis in *P. volubilis*, are therefore of great theoretical value.

In this study, the *PvFAD3* gene was obtained by PCR homologous cloning based on the transcriptome data of *P. volubilis* in our previous studies [21]. The bioinformatics analysis of PvFAD3 showed that the full-length DNA sequence of PvFAD3 was 1871 bp, including eight exons and seven introns, encoding 379 amino acids, with a molecular weight of 43.53 kDa and an isoelectric point of 7.79. The PvFAD3 cloned in this study was similar to that of *R. communis*, *J. curcas*, and *Hevea brasiliensis*, the members of Euphorbiaceae. The closer genetic distance of  $\omega$ -3 fatty acid dehydrogenase (FAD3) in the same family in the phylogenetic analysis indicated that the FAD3 was more conserved in the biological structure of species within the same family and with higher homology.

The structural analysis of the amino acid sequence of PvFAD3 protein showed that the C-terminus contained a distinct endoplasmic reticulum retention signal (KKLA motif), but there was no signal peptide or restriction enzyme cutting site. This finding supports the conclusion that the PvFAD3 protein is primarily localized to the endoplasmic reticulum via subcellular localization, as observed in tobacco leaf epidermis. McCartney et al. [36] reported that the C-terminal sequences rich in aromatic amino acids can localize fatty acid dehydrogenase to the endoplasmic reticulum membrane, and the C-terminal amino acid sequences of the  $\omega$ -3 fatty acid dehydrogenase (FAD3) of the 35 plants were rich in aromatic amino acids (Figure 2). In addition, the amino acid sequence of the PvFAD3 protein contained the "KKLA" sequence. To sum up, the PvFAD3 protein was a typical  $\omega$ -3 fatty acid dehydrogenase protein in the endoplasmic reticulum, that may bind tightly to the substrate and have a high catalytic efficiency, facilitating the conversion of linoleic acid to  $\alpha$ -linolenic acid. Based on the structural comparison of the amino acid sequences of the different species,  $\omega$ -3 fatty acid dehydrogenase of all 35 plant species had 3 specific histidine-conserved regions (Hisbox I, Hisbox II, and Hisbox III) that formed covalent bonds with amino acids embedded in the endoplasmic reticulum membrane and thus anchored to the endoplasmic reticulum. Only a few amino acid residues of plants in the conserved regions of Hisbox II and Hisbox III were changed. Predictably, the histidine-conserved regions in the  $\omega$ -3 fatty acid dehydrogenase were conserved and stable in higher plants; this finding is in accordance with the results of the analysis of the histidine-conserved regions of  $\omega$ -6 and  $\omega$ -3 fatty acid dehydrogenases by Guan et al. (2013) [28]. In the present study, the positions of the three histidine-conserved regions were annotated on the full-length sequence structure of the PvFAD3 (Figure 1), and all three histidine-conserved regions were located in the intron regions, with Hisbox I and Hisbox II in the first intron region and Hisbox III in the fourth intron region. This observation further confirmed that introns play a crucial role in ensuring the conserved function of the gene during the evolution of species [37].

The expression patterns of genes can provide direction for their functional roles. Several studies have confirmed that the FAD3 is highly expressed in nonphotosynthetic tissues such as roots, flowers, and seeds of nonoil plants, including *A. thaliana* [38], *Gossypium hirsutum* [39], and *Oryza sativa* [40]. In contrast, it was specifically highly expressed in the seeds of oil plants, such as *P. frutescens* [41], *G. max* [42], *L. usitatissimum* [14], and *A. hypogaea* [15], which are closely related to the biosynthesis of  $\alpha$ -linolenic acid in seeds. In the present study, the expression patterns of *PvFAD3* in different tissues such as roots, stems, leaves, seeds, and pericarp showed that *PvFAD3* was expressed in different

parts and was specifically upregulated in the rapid accumulation stage of seed oil. In contrast, the relative expression in the nonphotosynthetic roots was not significantly different from that in photosynthetic new leaves. Thus, the expression of *PvFAD3* may not be directly related to photosynthesis in different tissues.

*FAD3* is a key gene for  $\alpha$ -linolenic acid biosynthesis in plants, which catalyzes the formation of  $\alpha$ -linolenic acid from linoleic acid by introducing a third double bond between C15 and C16 of linoleic acid [43]. The study of expression patterns of the *FAD3* in different oilseed plants showed that the high content of ALA in plant seeds might have a stronger correlation with the expression activity of the *FAD3*. To explore the possible molecular mechanism by which *PvFAD3* positively regulates the biosynthesis of  $\alpha$ -linolenic acid, we investigated the regulating effects of *PvFAD3* on the expression levels of two stages of developing seeds (the initial stage, Pv-1 and the fast oil accumulation stage, Pv-2) in *P. volubilis*. The expression of *PvFAD3* was downregulated at Pv-1 and significantly upregulated at Pv-2, consistent with the dynamic change of  $\alpha$ -linolenic acid content at various stages of seed development [21], thus further demonstrating the close correlation between *PvFAD3* expression and  $\alpha$ -linolenic acid accumulation. To further validate the biological function of the *PvFAD3*, a vector overexpressing the *PvFAD3* was constructed and overexpressed in tobacco seeds, which significantly increased the content of  $\alpha$ -linolenic acid (2.13%), significantly decreased the content of linoleic acid (6.78%), and obviously increased the oil content (24.22%) and palmitic acid (2.77%). The stearic and oleic acid contents did not change significantly. This is consistent with the finding that the overexpression of the *FAD3* gene significantly increased  $\alpha$ -linolenic acid content in plants such as *P. frutescens* [44], *J. curcas* [14], *G. max* [13], *O. sativa* [40], and *L. esculentum* [12].

## 5. Conclusions

In conclusion, the full-length sequence of *PvFAD3* was successfully cloned and analyzed using bioinformatics. The gene was subcellularly localized to the endoplasmic reticulum, and overexpression of the *PvFAD3* gene in tobacco showed a significant increase in  $\alpha$ -linolenic acid content and oil content in transgenic plant seeds. Collectively, the *PvFAD3* gene of *P. volubilis* was confirmed as a key enzyme gene for  $\alpha$ -linolenic acid synthesis, thus indicating that the *PvFAD3* gene can be used for fatty acid fraction improvement in oilseed plants. The results of this study would help reveal the molecular mechanism of  $\alpha$ -linolenic acid biosynthesis in oil plants, provide a basis for further research on its regulatory mechanism, and develop a foundation for high yield and high quality of oil plants.

**Supplementary Materials:** The following supporting information can be downloaded at: <https://www.mdpi.com/article/10.3390/genes13030450/s1>, Figure S1: Amplification results of the fusion vector; Figure S2: Amplification results of the overexpression vector; Figure S3 (A–D): The genetic transformation of transgenic tobacco; (E): PCR detection of positive plants of transgenic tobacco; Table S1: Primers used in this research; Table S2: Alignment description of endoplasmic reticulum  $\omega$ -3 fatty acid desaturases.

**Author Contributions:** Conceptualization, G.L.; methodology, G.L. and Z.W.; software, X.S.; formal analysis, G.L.; investigation, L.G. and Y.P.; writing—original draft preparation, G.L.; writing—review and editing, G.L. and Z.W. All authors have read and agreed to the published version of the manuscript.

**Funding:** This research was financially supported by the GuangDong Basic and Applied Basic Research Foundation (Project Number: 2021A1515011021 and 2019A1515110168).

**Institutional Review Board Statement:** Not applicable.

**Informed Consent Statement:** Not applicable.

**Data Availability Statement:** Not applicable.

**Conflicts of Interest:** The authors declare no conflict of interest.

## Abbreviations

$\alpha$ -Linolenic acid (C18:3, ALA); Docosahexaenoic acid (DHA, C22:6); Eicosapentaenoic acid (EPA, C20:5);  $\omega$ -3 fatty acid desaturase (*FAD3*);  $\beta$ -Glucuronidase (GUS); Lys-Asp-Glu-Leu (KDEL); Lys-Lys-X-X (KKXX); kanamycin (Kan); Open reading frames (ORF); Theoretical isoelectric point (pI); phenylalanine (Phe, Y); real-time reverse transcription-polymerase chain reaction (qRT-PCR); Tyroxine (Tyr, Y).

## References

1. Bussmann, R.W.; Paniagua Zambrana, N.; Téllez, C. *Plukenetia carolis-vegae* (Euphorbiaceae)—A new useful species from northern Peru. *Econ. Bot.* **2013**, *67*, 387–392. [[CrossRef](#)]
2. Gutiérrez, L.-F.; Rosada, L.M.; Jiménez, Á. Chemical composition of Sacha Inchi (*Plukenetia volubilis* L.) seeds and characteristics of their lipid fraction. *Grasas Aceites* **2011**, *62*, 76–83. [[CrossRef](#)]
3. Chandrasekaran, U.; Liu, A. Stage-specific metabolization of triacylglycerols during seed germination of Sacha Inchi (*Plukenetia volubilis* L.). *J. Sci. Food Agric.* **2015**, *95*, 1764–1766. [[CrossRef](#)] [[PubMed](#)]
4. Wang, S.; Zhu, F.; Kakuda, Y. Sacha inchi (*Plukenetia volubilis* L.): Nutritional composition, biological activity, and uses. *Food Chem.* **2018**, *265*, 316–328. [[CrossRef](#)] [[PubMed](#)]
5. Feng, C.; Zhu, Y.; Zhang, T.; Bai, X.; He, H.; Pan, B.; Fu, Q.; Xu, Z. Analysis of nutritional components in tender stems and leaves of the woody oil crop *Plukenetia volubilis*. *Non-Wood For. Res.* **2021**, *39*, 97–103.
6. Kodahl, N. Sacha inchi (*Plukenetia volubilis* L.)—From lost crop of the Incas to part of the solution to global challenges? *Planta* **2020**, *251*, 80. [[CrossRef](#)]
7. Baker, E.J.; Miles, E.; Burdge, G.; Yaqoob, P.; Calder, P.C. Metabolism and functional effects of plant-derived omega-3 fatty acids in humans. *Prog. Lipid Res.* **2016**, *64*, 30–56. [[CrossRef](#)]
8. Yu, S.Y.; Zhang, X.; Huang, L.B.; Lyu, Y.P.; Zhang, Y.; Yao, Z.J.; Zhang, X.X.; Yuan, J.H.; Hu, Y.H. Transcriptomic analysis of  $\alpha$ -linolenic acid content and biosynthesis in *Paeonia ostii* fruits and seeds. *BMC Genom.* **2021**, *22*, 297. [[CrossRef](#)]
9. Berestovoy, M.; Pavlenko, O.S.; Goldenkova-Pavlova, I.V. Plant Fatty Acid Desaturases: Role in the Life of Plants and Biotechnological Potential. *Biol. Bull. Rev.* **2020**, *10*, 127–139. [[CrossRef](#)]
10. Puttick, D.; Dauk, M.; Lozinsky, S.; Smith, M.A. Overexpression of a *FAD3* Desaturase Increases Synthesis of a Polymethylene-Interrupted Dienoic Fatty Acid in Seeds of *Arabidopsis thaliana* L. *Lipids* **2009**, *44*, 753–757. [[CrossRef](#)]
11. Yang, Q.; Fan, C.; Guo, Z.; Qin, J.; Wu, J.; Li, Q.; Fu, T.; Zhou, Y. Identification of *FAD2* and *FAD3* genes in *Brassica napus* genome and development of allele-specific markers for high oleic and low linolenic acid contents. *Theor. Appl. Genet.* **2012**, *125*, 715–729. [[CrossRef](#)]
12. Domínguez, T.; Hernández, M.L.; Pennycooke, J.C.; Jiménez, P.; Martínez-Rivas, J.M.; Sanz, C.; Stockinger, E.J.; Sánchez-Serrano, J.J.; Sanmartín, M. Increasing  $\omega$ -3 desaturase expression in tomato results in altered aroma profile and enhanced resistance to cold stress. *Plant Physiol.* **2010**, *153*, 655–665. [[CrossRef](#)]
13. Pham, A.-T.; Shannon, J.G.; Bilyeu, K.D. Combinations of mutant *FAD2* and *FAD3* genes to produce high oleic acid and low linolenic acid soybean oil. *Theor. Appl. Genet.* **2012**, *125*, 503–515. [[CrossRef](#)]
14. Wu, P.; Zhang, S.; Zhang, L.; Chen, Y.; Li, M.; Jiang, H.; Wu, G. Functional characterization of two microsomal fatty acid desaturases from *Jatropha curcas* L. *J. Plant Physiol.* **2013**, *170*, 1360–1366. [[CrossRef](#)]
15. Wu, L.; Li, F.; Wu, X.; Song, D.; Wang, M. Cloning and expression characteristics of one  $\omega$ -3 cis 15 fatty acid dehydrogenase gene *AhFAD3A* in *Arachis hypogaea* L. *Chin. Oil Crop Sci.* **2015**, *37*, 41–47.
16. Lee, K.-R.; Lee, Y.; Kim, E.-H.; Lee, S.-B.; Roh, K.H.; Kim, J.-B.; Kang, H.-C.; Kim, H.U. Functional identification of oleate 12-desaturase and  $\omega$ -3 fatty acid desaturase genes from *Perilla frutescens* var. *frutescens*. *Plant Cell Rep.* **2016**, *35*, 2523–2537. [[CrossRef](#)]
17. Huang, X.; Lu, J.; Liao, B.; Bai, H.; Guan, L.; Zhang, T. Cloning and expression analysis of fatty acid desaturase gene *FAD3* from oil peony. *Sci. Agric. Sin.* **2017**, *50*, 1914–1921.
18. Wang, P.; Cao, H.; Chen, D.; Chen, D.; Chen, G.; Yang, J.; Ye, N. Cloning and Expression Analysis of Fatty Acid Desaturase Family Genes in *Camellia sinensis*. *Acta Hort. Sin.* **2020**, *47*, 1141–1152.
19. Bhunia, R.K.; Chakraborty, A.; Kaur, R.; Gayatri, T.; Bhattacharyya, J.; Basu, A.; Maiti, M.; Sen, S.K. Seed-specific increased expression of 2S albumin promoter of sesame qualifies it as a useful genetic tool for fatty acid metabolic engineering and related transgenic intervention in sesame and other oil seed crops. *Plant Mol. Biol.* **2014**, *86*, 351–365. [[CrossRef](#)]
20. Feng, Y.Z. *Transcriptome Sequencing and Study on FAD3 Gene Identification and Function in Eucommia Ulmoides Oliv*; Chinese Academy of Forestry: Beijing, China, 2016.
21. Liu, G.; Wu, Z.; Peng, Y.; Shang, X.; Xie, Y.; Arnold, R.J. Transcriptome analyses reveals the dynamic nature of oil accumulation during seed development of *Plukenetia volubilis* L. *Sci. Rep.* **2020**, *10*, 20467. [[CrossRef](#)]
22. Wang, X.; Liu, A. Expression of Genes Controlling Unsaturated Fatty Acids Biosynthesis and Oil Deposition in Developing Seeds of Sacha Inchi (*Plukenetia volubilis* L.). *Lipids* **2014**, *49*, 1019–1031. [[CrossRef](#)]
23. Wang, X.; Xu, R.; Wang, R.; Liu, A. Transcriptome analysis of Sacha Inchi (*Plukenetia volubilis* L.) seeds at two developmental stages. *BMC Genom.* **2012**, *13*, 716. [[CrossRef](#)]

24. Livak, K.J.; Schmittgen, T.D. Analysis of relative gene expression data using real-time quantitative PCR and the  $2^{-\Delta\Delta Ct}$  Method. *Methods* **2001**, *25*, 402–408. [[CrossRef](#)]
25. Nelson, B.K.; Cai, X.; Nebenführ, A. A multicolored set of in vivo organelle markers for co-localization studies in Arabidopsis and other plants. *Plant J.* **2007**, *51*, 1126–1136. [[CrossRef](#)]
26. Liu, G.; Chen, H.P.; Peng, Y.; Xie, Y.J.; Chen, S.X. Variations in fatty acid composition of Sacha inchi seeds during growth and development. *China Oils Fats* **2018**, *43*, 57–62.
27. Shanklin, J.; Whittle, E.; Fox, B.G. Eight Histidine Residues Are Catalytically Essential in a Membrane-Associated Iron Enzyme, Stearoyl-CoA Desaturase, and Are Conserved in Alkane Hydroxylase and Xylene Monooxygenase. *Biochemistry* **1994**, *33*, 12787–12794. [[CrossRef](#)]
28. Guan, L.; Hou, K.; Chen, J.; Xu, Y.; Wu, W. Phylogenetic and functional differentiation of the omega-6 and omega-3 fatty acid dehydrogenase families. *Hereditas* **2013**, *35*, 643–654.
29. Czumaj, A.; Śledziński, T. Biological role of unsaturated fatty acid desaturases in health and disease. *Nutrients* **2020**, *12*, 356. [[CrossRef](#)] [[PubMed](#)]
30. Yang, Y.; Wang, G.; Pan, X. *China Food Composition*, 2nd ed.; Peking University Medical Press: Beijing, China, 2009.
31. Shen, Q.; Zhu, W.X.; Qin, X.R.; Zhao, Y.; Wang, X.P.; Li, M.; Du, C.F. Oil Content and fatty acid components of 30 *Perilla frutescens* samples in Guizhou. *Guizhou Agric. Sci.* **2014**, *42*, 5–8.
32. Porrás-Loaiza, P.; Jiménez-Munguía, M.T.; Sosa-Morales, M.E.; Palou, E.; López-Malo, A. Physical properties, chemical characterization and fatty acid composition of Mexican chia (*Salvia hispanica* L.) seeds. *Int. J. Food Sci. Technol.* **2014**, *49*, 571–577. [[CrossRef](#)]
33. Xing, L.; Zhao, F.-M.; Cao, Y.-F.; Wang, M.; Mei, S.; Li, S.-P.; Cai, Z.-Y. Principal component analysis of mineral elements and fatty acids composition in flaxseed from ten different regions. *Spectrosc. Spectr. Anal.* **2014**, *34*, 2538–2543.
34. Kodahl, N.; Sørensen, M. Sacha Inchi (*Plukenetia volubilis* L.) Is an Underutilized Crop with a Great Potential. *Agronomy* **2021**, *11*, 1066. [[CrossRef](#)]
35. Li, S.-S.; Wang, L.-S.; Shu, Q.-Y.; Wu, J.; Chen, L.-G.; Shao, S.; Yin, D.-D. Fatty acid composition of developing tree peony (*Paeonia* section Moutan DC.) seeds and transcriptome analysis during seed development. *BMC Genom.* **2015**, *16*, 208. [[CrossRef](#)]
36. McCartney, A.W.; Dyer, J.M.; Dhanoa, P.K.; Kim, P.K.; Andrews, D.W.; McNew, J.A.; Mullen, R.T. Membrane-bound fatty acid desaturases are inserted co-translationally into the ER and contain different ER retrieval motifs at their carboxy termini. *Plant J.* **2004**, *37*, 156–173. [[CrossRef](#)]
37. Long, M.; Rosenberg, C.; Gilbert, W. Intron phase correlations and the evolution of the intron/exon structure of genes. *Proc. Natl. Acad. Sci. USA* **1995**, *92*, 12495–12499. [[CrossRef](#)]
38. Matsuda, O.; Watanabe, C.; Iba, K. Hormonal regulation of tissue-specific ectopic expression of an Arabidopsis endoplasmic reticulum-type  $\omega$ -3 fatty acid desaturase (FAD3) gene. *Planta* **2001**, *213*, 833–840. [[CrossRef](#)]
39. Feng, J.; Dong, Y.; Liu, W.; He, Q.; Daud, M.K.; Chen, J.; Zhu, S. Genome-wide identification of membrane-bound fatty acid desaturase genes in *Gossypium hirsutum* and their expressions during abiotic stress. *Sci. Rep.* **2017**, *7*, srep45711. [[CrossRef](#)]
40. Liu, H.L.; Yin, Z.J.; Xiao, L.; Xu, Y.N.; Qu, L.Q. Identification and evaluation of  $\omega$ -3 fatty acid desaturase genes for hyperfortifying  $\alpha$ -linolenic acid in transgenic rice seed. *J. Exp. Bot.* **2012**, *63*, 3279–3287. [[CrossRef](#)]
41. Xue, Y.; Chen, B.; Win, A.N.; Fu, C.; Lian, J.; Liu, X.; Wang, R.; Zhang, X.; Chai, Y. Omega-3 fatty acid desaturase gene family from two  $\omega$ -3 sources, *Salvia hispanica* and *Perilla frutescens*: Cloning, characterization and expression. *PLoS ONE* **2018**, *13*, e0191432. [[CrossRef](#)]
42. Román, Á.; Andreu, V.; Hernández, M.L.; Lagunas, B.; Picorel, R.; Martínez-Rivas, J.M.; Alfonso, M. Contribution of the different omega-3 fatty acid desaturase genes to the cold response in soybean. *J. Exp. Bot.* **2012**, *63*, 4973–4982. [[CrossRef](#)]
43. Duan, W.; Lijun, W.; Shimei, Y.; Shen, Q.; Zhao, D. Advances on formation and regulation mechanism of  $\alpha$ -linolenic acid in seeds. *J. Plant Genet. Resour.* **2020**, *21*, 49–62.
44. Wu, D.; Yang, S.M.; Shang, Z.W.; Xu, J.; Zhao, D.G.; Wang, H.B.; Shen, Q. Genome-wide analysis of the fatty acid desaturase gene family reveals the key role of PffAD3 in  $\alpha$ -linolenic acid biosynthesis in *Perilla* Seeds. *Front. Genet.* **2021**, *12*, 735862.